

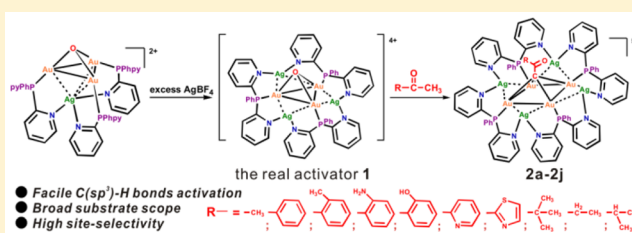
Highly Active Gold(I)–Silver(I) Oxo Cluster Activating sp^3 C–H Bonds of Methyl Ketones under Mild Conditions

Xiao-Li Pei, Yang Yang, Zhen Lei, Shan-Shan Chang, Zong-Jie Guan, Xian-Kai Wan, Ting-Bin Wen, and Quan-Ming Wang*

State Key Lab of Physical Chemistry of Solid Surfaces, Collaborative Innovation Center of Chemistry for Energy Materials (iChem), Department of Chemistry, College of Chemistry and Chemical Engineering, Xiamen University, Xiamen 361005, Fujian, P. R. China

S Supporting Information

ABSTRACT: The activation of $C(sp^3)$ –H bonds is challenging, due to their high bond dissociation energy, low proton acidity, and highly nonpolar character. Herein we report a unique gold(I)–silver(I) oxo cluster protected by hemilabile phosphine ligands $[O Au_3 Ag_3 (PPhpy_2)_3] (BF_4)_4$ (**1**), which can activate $C(sp^3)$ –H bonds under mild conditions for a broad scope of methyl ketones ($RCOCH_3$, R = methyl, phenyl, 2-methylphenyl, 2-aminophenyl, 2-hydroxyphenyl, 2-pyridyl, 2-thiazolyl, *tert*-butyl, ethyl, isopropyl). Activation happens via triple deprotonation of the methyl group, leading to formation of heterometallic Au(I)–Ag(I) clusters with formula $RCO Au_4 Ag_4 (PPhpy_2)_4 (BF_4)_5$ ($PPhpy_2$ = bis(2-pyridyl)phenylphosphine). Cluster **1** can be generated *in situ* via the reaction of $[O Au_3 Ag (PPhpy_2)_3] (BF_4)_2$ with 2 equiv of $AgBF_4$. The oxo ion and the metal centers are found to be essential in the cleavage of sp^3 C–H bonds of methyl ketones. Interestingly, cluster **1** selectively activates the C–H bonds in $-CH_3$ rather than the N–H bonds in $-NH_2$ or the O–H bond in $-OH$ which is traditionally thought to be more reactive than C–H bonds. Control experiments with butanone, 3-methylbutanone, and cyclopentanone as substrates show that the auration of the C–H bond of the terminal methyl group is preferred over secondary or tertiary sp^3 C–H bonds; in other words, the C–H bond activation is influenced by steric effect. This work highlights the powerful reactivity of metal clusters toward C–H activation and sheds new light on gold(I)-mediated catalysis.



- Facile $C(sp^3)$ -H bonds activation
- Broad substrate scope
- High site-selectivity

INTRODUCTION

C–H activation of small molecules by transition-metal complexes has experienced rapid growth recently.^{1–4} Gold(I) species as a powerful π -acid is considered to be one of the most important catalysts in homogeneous catalysis.^{5–8} Methodologies for aromatic $C(sp^2)$ –H activation by Au(I) have been extensively developed, and usually employ the synergic action of electrophilic Au(I) and auxiliary base ligands^{9,10} to lower the C–H activation energy.¹¹ In contrast, $C(sp^3)$ –H activation has advanced much more slowly because of its high bond dissociation energy, low proton acidity, and highly nonpolar character.² Thus, it is challenging to activate the $C(sp^3)$ –H bond under mild conditions.

Methyl ketones are widely used in organic synthesis^{12,13} and catalysis,^{14,15} so an efficient method for $C(sp^3)$ –H activation of methyl ketones is of great interest in terms of both fundamental studies and potential applications. Gold(I)-mediated $C(sp^3)$ –H activation of ketones is rare,^{16–18} despite the lack of known transition-metal-mediated C–H activation of ketones.^{19–24} To our knowledge, no previous examples of gold(I)-mediated C–H bond activation of ketones to generate triply deprotonated methyl ketones have been reported. Herein, we demonstrate that a new gold(I)–silver(I) oxo cluster $[O Au_3 Ag_3 (PPhpy_2)_3] (BF_4)_4$ (**1**) ($PPhpy_2$ = bis(2-pyridyl)phenylphosphine) can activate $C(sp^3)$ –H bonds of a broad scope of methyl ketones

under mild conditions, leading to the formation of a series of novel geminal tetraaurated methyl ketones $[RCO Au_4 Ag_4 (PPhpy_2)_4] (BF_4)_5$ (R = methyl, **2a**; phenyl, **2b**; 2-methylphenyl, **2c**; 2-aminophenyl, **2d**; 2-hydroxyphenyl, **2e**; 2-pyridyl, **2f**; 2-thiazolyl, **2g**; *tert*-butyl, **2h**; ethyl, **2i**; isopropyl, **2j**). We show further that **1** can be generated *in situ* by introducing 2 equiv of $AgBF_4$ into $[O Au_3 Ag (PPhpy_2)_3] (BF_4)_2$ (**3**).

RESULTS AND DISCUSSION

Synthesis and Characterization. Our story started with acetone, the simplest methyl ketone. The interesting reactivity of heterometallic Au(I)–Ag(I) oxo clusters with acetone was discovered serendipitously. Acetone was initially used as a solvent to perform the addition of silver ions to **3** in order to prepare a luminescent heterometallic cluster in view of the remaining coordinating ability of $PPhpy_2$,²⁵ but unexpectedly acetone turned out to be a reactant involved in C–H activation. The preparation of **3** (see Supporting Information) is similar to that of $[O Au_3 Ag (dppy)_3] (BF_4)_2$.²⁶ The treatment of **3** with 2 equiv of $AgBF_4$ in acetone at room temperature resulted in a gradual change of solution color from colorless to red; after

Received: February 15, 2015

Published: April 6, 2015

about 4 h the red solution was evaporated to dryness to yield a crude red solid. This solid was recrystallized to afford red block crystals of **2a** in 76% yield. ^{31}P NMR in CD_3CN showed a singlet at 38 ppm, reflecting the high symmetry of $[\text{CH}_3\text{COC-Au}_4\text{Ag}_4(\text{PPhpy}_2)_4]^{5+}$ due to rotation of the single C–C bond of the triply deprotonated acetone, $\text{CH}_3\text{COC}^{3-}$, in solution. The ^{13}C NMR spectrum of **2a** in CD_3CN revealed a singlet at 214.29 ppm, which is assigned to the quaternary carbon atom of carbonyl. This signal is significantly downfield shifted in comparison with that of acetone, 19,21 due to the withdrawing effect by the adjacent tetraaurated methyl group. ^{31}P NMR, ^1H NMR, ^{13}C NMR, HSQC, COSY, and IR spectra support the composition and structure of **2a** as determined by X-ray diffraction (see Supporting Information).

X-ray crystallographic analysis 27 revealed that the cation $[\text{CH}_3\text{COC-Au}_4\text{Ag}_4(\text{PPhpy}_2)_4]^{5+}$ of **2a** features a square pyramidal structure composed of four $[\text{LAu}]^+$ units ($\text{L} = \text{PPhpy}_2$) with a hypercoordinated $\text{CH}_3\text{COC}^{3-}$ group at the apex (Figure 1). Four $\text{Ag}(\text{I})$ ions are linked to the

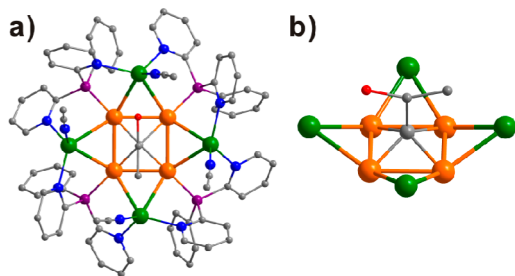


Figure 1. (a) Top view of the cation in **2a**. (b) Structure of the $\text{CH}_3\text{COC-Au}_4\text{Ag}_4$ unit in **2a**. Color code: orange, Au; green, Ag; purple, P; blue, N; red, O; grey, C.

$\text{CH}_3\text{COC-Au}_4$ moiety through the bridging PPhpy_2 ligands, forming $\text{Au}(\text{I})\cdots\text{Ag}(\text{I})$ metallophilic interactions. Each $\text{Ag}(\text{I})$ ion is additionally ligated by a N donor from acetonitrile (Figure 1a). The $\text{Au}(\text{I})\cdots\text{Au}(\text{I})$ and $\text{Au}(\text{I})\cdots\text{Ag}(\text{I})$ distances are 2.7947(8) and 2.8914(17) Å, respectively. The C–Au–P arrangement is close to linear, with a bond angle of $172.6(8)^\circ$. The Au–C–Au angle of two neighboring gold atoms is $81.3(7)^\circ$. $\text{Au}(\text{I})$ complexes containing a similar tetragold motif have been reported previously, such as $[\text{Au}_8\text{L}_8]^{2+}$ ($\text{L} = \text{P}(\text{mesityl})_3$), 28 $[\text{H}_3\text{C-C}(\text{AuL})_4]^+$ ($\text{L} = \text{PPh}_3$, $\text{P}(\text{C}_6\text{H}_{11})_3$, $\text{L}_2 = 1,2\text{-C}_6\text{H}_4(\text{CH}_2\text{CH}_2\text{PPh}_2)_2$), 29 $[(\text{RC})(\text{AuL})_4]^+$ ($\text{R} = \text{H}$, $\text{L} = \text{PPh}_3$, 30 $\text{R} = \text{SOMe}_2$, $\text{L} = \text{PPh}_3$), 31 $[(\text{RC-AuL}_3)_2]^{2+}$ ($\text{R} = \text{oxazoliny}$, $\text{L} = \text{PPh}_3$), 32 and $[(\text{RC})_2\text{Au}_8\text{L}_4]^{2+}$ ($\text{R} = \text{PPh}_2\text{Me}$, $\text{L} = \text{CH}(\text{NC}_8\text{H}_9)_2$), 33 $\text{R} = \text{PhCO}$, $\text{L} = \text{PPh}_2\text{C}_6\text{H}_4\text{PPh}_2$). 34 It is worth noting that $[(\mu_4\text{-CSOMe}_2)(\text{AuPPh}_3)_4]^+$ was obtained by the auration of $[\text{Me}_3\text{S=O}]\text{ClO}_4$ with $[\text{Au}(\text{acac})\text{PPh}_3]$ (acac = acetylacetonato) in acetone, 31 where acetone did not undergo any reaction with $[\text{Au}(\text{acac})\text{PPh}_3]$.

Active Species. As acetone is often used as a solvent in the preparation of $\text{Au}(\text{I})$ and $\text{Au}(\text{I})/\text{Ag}(\text{I})$ oxonium clusters, $^{26,35-38}$ the reaction of acetone with **3**/ AgBF_4 is unusual. In order to identify the active species in the $\text{C}(\text{sp}^3)\text{-H}$ bond activation of acetone, a series of experiments were carried out (Table 1). No reaction between **3** and acetone occurred, as the ^{31}P NMR spectrum of **3** in d_6 -acetone showed no obvious change for hours (entry 1). When 2 equiv of AgBF_4 was involved in the reaction (entry 2), crystals of **2a** could be isolated in 76% yield. Because each PPhpy_2 ligand has two pyridyl groups, cluster **3** has extra N donors available for binding of additional silver

Table 1. Various Conditions for Acetone C–H Activation a

entry	[Au]	[Ag]	yield c (%)
1	$[\text{OAu}_3\text{Ag}(\text{PPhpy}_2)_3](\text{BF}_4)_2$ (3)		0
2	$[\text{OAu}_3\text{Ag}(\text{PPhpy}_2)_3](\text{BF}_4)_2$ (3)	AgBF_4	76
3	$[\text{OAu}_3\text{Ag}_3(\text{PPhpy}_2)_3](\text{BF}_4)_4$ (1) b		70
4	$\text{PPhpy}_2\text{AuCl}$	AgBF_4	0
5	$\text{PPhpy}_2\text{AuCl}$	$\text{Ag}_2\text{O}/\text{AgBF}_4$	75
6		Ag_2O	0
7		$\text{Ag}_2\text{O}/\text{AgBF}_4$	0
8	$[\text{OAu}_3\text{Ag}(\text{dppy})_3](\text{BF}_4)_2$	AgBF_4	0
9	dppyAuCl	$\text{Ag}_2\text{O}/\text{AgBF}_4$	0

a All reactions use acetone as the solvent. b A 2 equiv portion of AgBF_4 was added into the suspension of **3** in methanol, and then the mixture was stirred for 30 min at room temperature. The resulting suspension was isolated by centrifugal sedimentation, and milky solid was obtained as complex **1**. c Crystal isolation yield of **2a** (based on gold).

ions. When 2 equiv of AgBF_4 was reacted with **3** in methanol instead of in acetone, no C–H activation was observed; a milky solid was formed which was found to be **1** (*vide infra*). Simply dissolving **1** in acetone led to the generation of **2a** as well as the observation of a color change, and the isolation yield of **2a** crystals is 70%! These facts suggest that **1** is the active species responsible for the C–H activation of acetone.

No color change was observed for the mixture of $\text{PPhpy}_2\text{AuCl}$ and AgBF_4 in acetone (entry 4 in Table 1); the ^{31}P NMR spectrum only showed a peak at 31 ppm corresponding to $\text{PPhpy}_2\text{Au}(\text{BF}_4)$, indicating no activation. When Ag_2O was involved in the reaction (entry 5), the reaction mixture turned red, and a singlet at 38 ppm appeared in ^{31}P NMR, indicating the formation of **2a**. The isolation yield of red crystals of **2a** could be up to 75%. Because the reaction of $\text{PPhpy}_2\text{AuCl}$ with Ag_2O in methanol gave **3**, entry 5 is identical to entry 2. 26 No reaction with acetone was observed with simple silver salts as shown in entries 6 and 7. These data provide additional evidence that **1** is the active species.

The composition of **1** obtained from the reaction of **3** and AgBF_4 in methanol was first studied by EDX, which showed that the Au:Ag molar ratio was roughly 1:1. Considering the presence of free N donors from PPhpy_2 in **3**, we presumed that **1** has a composition of $[\text{OAu}_3\text{Ag}_3(\text{PPhpy}_2)_3](\text{BF}_4)_4$. DFT optimization gave a structure of $[\text{OAu}_3\text{Ag}_3(\text{PPhpy}_2)_3]^{4+}$ as shown in Figure 2. Definitive evidence came from the X-ray structural analysis of an analogue of **1**. Although the crystallization of **1** failed due to its poor solubility in CH_2Cl_2 and high activity in other soluble solvents such as CH_3CN and DMSO, the structural determination of $[\text{OAu}_3\text{Ag}_3(\text{PPh}(5\text{-Mepy})_2)_3](\text{BF}_4)_4$ (**4**), where $\text{PPh}(5\text{-Mepy})_2$ is bis(*S*-methyl-2-pyridyl)phenylphosphine, was successful. Cluster **4** has a better

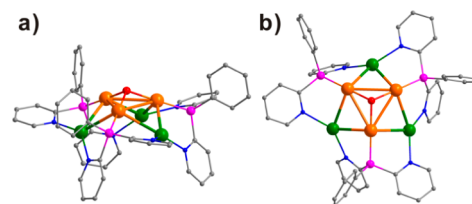


Figure 2. DFT-optimized structure of $[\text{OAu}_3\text{Ag}_3(\text{PPhpy}_2)_3]^{4+}$ in **1**: (a) side view, (b) top view. Selected DFT-optimized bond distances (Å): Au–Au, 3.275–3.284; Au–Ag, 3.035–3.056; P–Au, 2.308–2.309; N–Ag, 2.326–2.350; O–Au, 2.060.

solubility in CH_2Cl_2 than **1** does, due to the methyl groups in $\text{PPh}(\text{S-Mepy})_2$ ligands. As shown in Figure 3,³⁹ cluster **4**

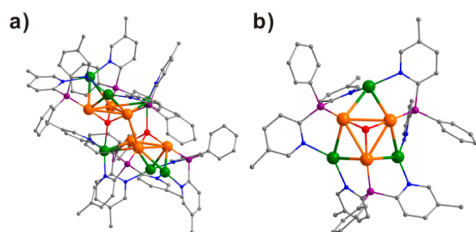


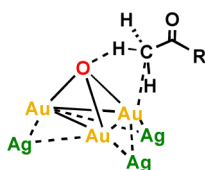
Figure 3. (a) Dimeric structure in $[\text{O}(\text{Au}_3\text{Ag}_3)(\text{PPh}(\text{S-Mepy})_2)_3(\text{BF}_4)_4]_2$ (**4**); (b) top view of a single cluster $[\text{O}(\text{Au}_3\text{Ag}_3)(\text{PPh}(\text{S-Mepy})_2)_3]^{4+}$ in **4**. Selected bond distances: Au...Au, 3.0393(9)–3.1477(9); Au...Ag, 2.8876(15)–3.0853(16); P–Au, 2.210(5)–2.227(3); N–Ag, 2.220(14)–2.326(8); O–Au, 2.058(12)–2.081(9); O–Ag, 2.436(11).

consists of an oxo-capped Au_3 triangle with three $\text{Ag}(\text{I})$ attached via the bridging phosphine ligands. The two $\text{O}(\text{Au}_3\text{Ag}_3)$ units dimerize through two intercluster O–Ag bonds and one Au...Au contact. The coordination mode of the oxonium ion $[\text{O}(\text{Au}_3\text{Ag})]$ is rare, which is similar to the $[\text{O}(\text{Au}_4)]$ unit in $[\text{O}(\text{Au}_4\text{L}_4)]^{2+}$ (L = tris(*o*-tolyl)phosphine).⁴⁰

It is worth noting that, under identical conditions, the cluster $[(\text{dppy})_3\text{O}(\text{Au}_3\text{Ag})](\text{BF}_4)_2$ (dppy = diphenylphosphino-2-pyridine)²⁵ cannot activate acetone as shown in entries 8 and 9. Due to the different coordination ability, the reaction with dppy could only generate $\text{O}(\text{Au}_3\text{Ag})$ rather than $\text{O}(\text{Au}_3\text{Ag}_3)$ as in the case of PPhpy_2 .

Proposed Mechanism. On the basis of the structure of **1** and above-mentioned observations, we propose that the C–H bond activation of acetone undergoes a concerted metalation/deprotonation process¹¹ as illustrated in Scheme 1. This

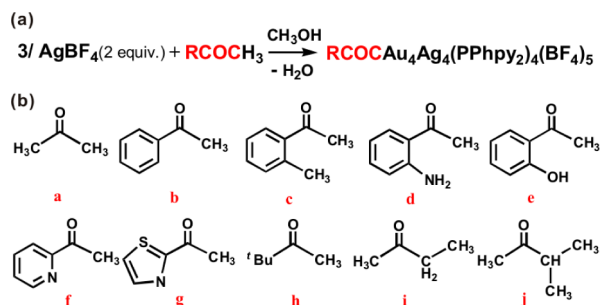
Scheme 1. Proposed Mechanism for C–H Activation by **1**



mechanism is slightly different from that of the activation of CH_3CN with $[(\text{dppy})_3\text{O}(\text{Au}_3\text{Ag})](\text{BF}_4)_2$ where protic solvent such as methanol is involved in the activation.⁴¹ Scheme 1 shows that Au(I) attacks the methyl carbon of acetone, while the oxo ion interacts with a methyl hydrogen. Gold and carbon have similar electronegativities,⁴² which facilitate formation of Au–C bonds with covalent characters. This is an important driving force for the activation. The oxo ion is also very important in the C–H bond cleavage process. It reacts with the methyl hydrogen atoms of acetone to form H_2O , thereby driving C–H bond activation. Silver ions make a critical contribution to the activity of **1**, as the attachment of silver ions to the gold oxo cluster results in more positive **1** (4+) in comparison to the nonactive **3** (2+). Higher positive charge enhances the binding between gold(I) and the methyl carbon of acetone. In addition, the pronounced tendency of gold atoms to cluster around a given carbon center (as in CAu_5^+ , CAu_6^{2+} , and HCAu_4^+)⁴³ also helps the activation by forming the final tetrauration cluster.

Substrate Scope. To go beyond C–H bond activation of acetone, we expanded the scope of the protocol by applying **1** to other methyl ketones. Methanol was chosen as the solvent, because of its inertness to **1**. The reactions were generalized as shown in Scheme 2a. Investigated methyl ketones include

Scheme 2. (a) C–H Activation Reaction Scheme of Methyl Ketones and (b) Various Methyl Ketones Used



acetophenone, 2'-methylacetophenone, 2-aminoacetophenone, 2'-hydroxyacetophenone, 2-acetylpyridine, 2-acetylthiazole, pinacolone, butanone, and 3-methylbutanone (Scheme 2b). In each case, the addition of a methyl ketone in a methanol solution containing 2 equiv of AgBF_4 and 1 equiv of **3** led to the formation of the corresponding C–H activation product: the ketone was triply deprotonated to generate RCOC^{3-} , which was stabilized in the heterometallic cluster $[\text{RCO}(\text{CAu}_4\text{Ag}_4)(\text{PPhpy}_2)_4]^{5+}$. The reactions for **2b,d–g** went smoothly at room temperature, while longer reaction time and higher temperature (70 °C) were required for **2c,h–j** due to poor solubility of **1** in 2'-methylacetophenone, pinacolone, butanone, and 3-methylbutanone in methanol.

All tetraaurated methyl ketones from Scheme 2 were isolated as red crystals in good yield and structurally determined by single crystal X-ray diffraction⁴⁴ (Figure 4). They all have a very similar square pyramidal structure, comprising a Au_4 square and a $\mu_4\text{-RCOC}^{3-}$ ligand as the apex as well as four attaching silver atoms. Due to different solvents used in crystallization, the four silver ions are coordinated by different solvent molecules: four MeCN in **2a–c,h,i**; three MeCN in **2e,g**; two MeCN and one H_2O in **2d**; three MeCN in **2f**; three MeCN and one H_2O in **2j**. In **2b**, additional coordination to silver atoms from an oxygen atom of a benzoyl group was found. A similar coordination mode was also observed in **2e,g,h**. Moreover, nitrogen donors from methyl ketones are linked to silver atoms in **2d,f,g**.

In the solid state, the environments of phosphorus atoms are not equivalent, but the ³¹P NMR spectra of **2b–j** in CD_3CN showed similar single resonances at about 37 ppm due to the rotation of $\mu_4\text{-RCOC}^{3-}$ along a C–C single bond. Interestingly, the ¹H NMR signals of hydrogen atoms in $-\text{NH}_2$ and $-\text{OH}$ were found at 4.99 and 12.78 ppm, respectively, for both in **2d** and **2e**, indicating that the N–H and O–H bonds were not aminated, despite the fact that $-\text{NH}_2$ and $-\text{OH}$ groups are quite reactive to oxonium gold(I) complexes.^{45–47} On the contrary, tetrauration happened at the methyl groups of 2-aminoacetophenone and 2'-hydroxyacetophenone, as shown in the structure of **2d** and **2e**. The exclusive auration of the $-\text{CH}_3$ group, leaving the $-\text{OH}$ or $-\text{NH}_2$ group nonmetalated, is probably due to the fact that the formation of Au–C bonds with low polarity is irreversible, while the formation of the more polar Au–N and Au–O bonds is reversible.^{48–50}

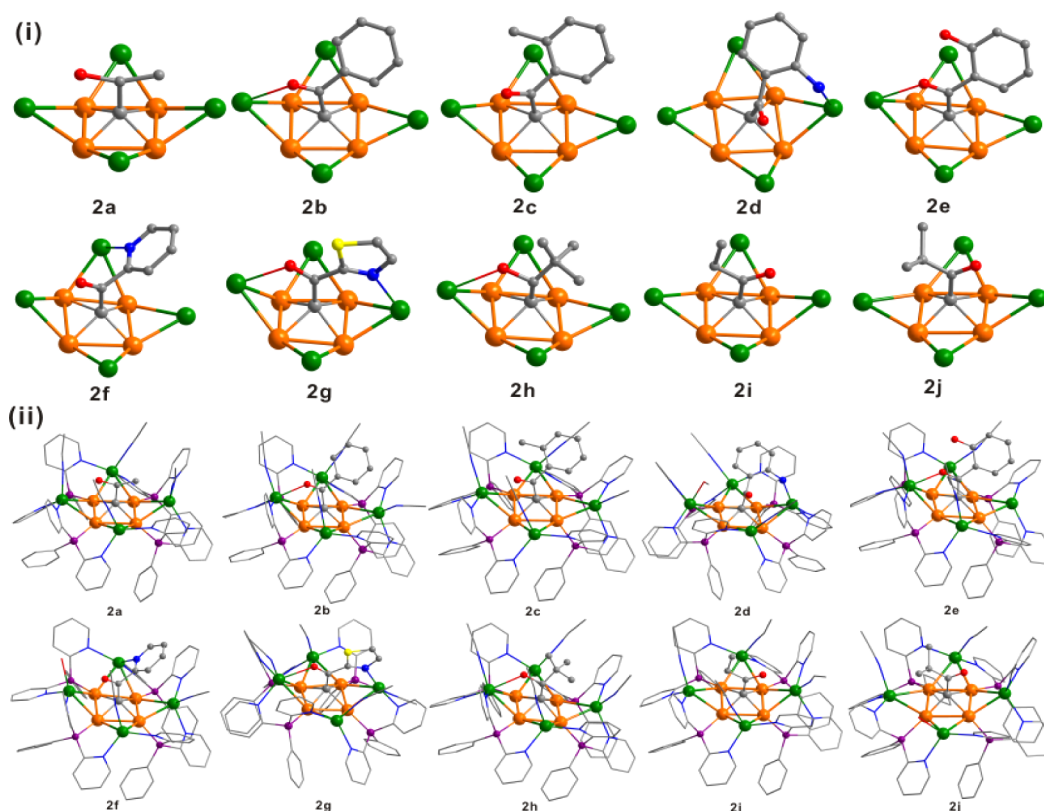


Figure 4. (i) RCOCAu₄Ag₄ skeletons in **2a–j**; (ii) structures of the [RCOCAu₄Ag₄(PPhpy₂)₄]⁵⁺ clusters in **2a–j**. Color code: orange, Au; green, Ag; yellow, S; purple, P; blue, N; red, O; gray, C.

The site-selectivity among primary, secondary, and tertiary C–H bonds was also evaluated with application of the protocol to butanone and 3-methylbutanone, leading to the isolation of **2i** and **2j**. The yield of **2i** was relatively low (~33%), which is ascribed to the competitive reaction from the CH₂ group of butanone. This was confirmed with a control experiment with 3-methylbutanone. The methyl group at the CH group increases the steric hindrance, so the competition is inhibited; as a result, the tetrauration product **2j** was isolated with a significantly higher yield (~63%). The C–H activation at secondary C–H bonds in ketones was further proven by reaction between 3/AgBF₄ and cyclopentanone, which gave a mixture containing **5**. Mass spectrometry showed (see in Supporting Information Figure S39) a dominant peak at *m/z* = 1005.14, corresponding to molecular ion [(CH₂CHCOCH₂CH₂)Au₂(PC₆H₅C₁₀H₈N₂)₂]⁺. This supports that C–H bond activation of CH₂ in a ketone may also take place.

CONCLUSION

We have demonstrated that the novel gold(I)–silver(I) oxo cluster **1** is very active in the C(sp³)–H bond cleavage of methyl ketones, resulting in the triple deprotonation of the methyl group. Heterometallic clusters containing geminal tetraaurated methyl ketones, RCOCAu₄Ag₄(PPhpy₂)₄(BF₄)₅, have been isolated in high yield. The activation can be performed under mild conditions. The affinity between gold and carbon as well as the deprotonation by oxo ions present important driving forces in the activation reactions. Silver ions contribute to the activity of **1** by increasing the cluster charge, as higher positive charge enhances the binding between gold(I)

and the methyl carbon of ketones. This work highlights the powerful reactivity of Au(I)–Ag(I) clusters toward C–H activation. Their ability to activate C(sp³)–H under mild conditions suggests a new alternative to C–H activation by leveraging multimetallic components or heterometallic clusters. This insight could lead to design of new cluster agents for activation of inert bonds.

EXPERIMENTAL SECTION

Reagents. All commercially available reagents were used without further purification. 2-Bromopyridine (99%), *n*-BuLi (1.6 M hexane solution), dichlorophenylphosphine (98%), silver tetrafluoroborate (99%, 55.4% Ag), acetophenone (98%), 2'-methylacetophenone (98%), and 2-acetylthiazole (99%) were purchased from J&K Chemical. 2-Acetylpyridine (98%) was purchased from Alfa Aesar Chemical Reagent Co. Ltd. 2-Aminoacetophenone (98%), 2'-hydroxyacetophenone (>98.0%), and 3-methyl-2-butanone (99%) were purchased from TCI (Shanghai) Development Co. Ltd. Pinacolone (97%) was purchased from Admas-beta Co. Ltd. (Shanghai). Cyclopentanone (>99.0%) was purchased from Aladdin Reagent Inc. 2-Butanone (analytical grade), acetone (analytical grade), acetonitrile (analytical grade), and methanol (analytical grade) were purchased from Sinopharm Chemical Reagent Co. Ltd. (Shanghai). The synthesis of PPhpy₂ was carried out under dry nitrogen atmosphere using Schlenk techniques according to literature procedures.⁵¹

Synthesis of 2a. To a solution of **3** [OAu₃Ag(PPhpy₂)₃](BF₄)₂ (337.2 mg, 0.20 mmol) in acetone (10 mL) was added 2 equiv of AgBF₄. The mixture was then stirred at room temperature for 4 h. The resulting red solution was evaporated to dryness to give a crude red solid. This solid was recrystallized by diffusion of diethyl ether into its solution in acetonitrile/acetone 1:3 (v/v) to afford 311 mg of **2a** as red block-like crystals after a week (yield 76%, based on gold).

Synthesis of 2b,d–g. The synthetic procedure was similar to that of 2a. To a suspension of 3 (60 mg) in MeOH (3 mL) was added 2 equiv of AgBF₄, and then excess ketone (100 μL) was added. One of the following was added for its appropriate product, respectively: acetophenone, 2'-hydroxyacetophenone, 2-aminoacetophenone, 2-acetylpyridine, and 2-acetylthiazole. The mixture was stirred at room temperature until a red solution was formed (2b, 6 h; 2d, 4 h; 2e, 4 h; 2f, 4 h; 2g, 4 h). After the solvent was evaporated, the oil residue was triturated with ether under ultrasonication to give a red solid. The crude product was dissolved in MeOH/MeCN (3 mL/0.3 mL), and after filtration, 5 mL of Et₂O was layered onto the filtrate. Red crystals suitable for X-ray analysis were formed after 2 weeks. Crystal isolation yields (based on gold): 2b, 49.2 mg, 65%; 2d, 50.3 mg, 66%; 2e, 50.1 mg, 64%; 2f, 62.2 mg, 80%; 2g, 58.5 mg, 75%.

Synthesis of 2c,h–j. The synthesis was similar to that for 2a but at higher temperature and longer reaction time. To a suspension of 3 (60 mg) in MeOH (3 mL) was added 2 equiv of AgBF₄, and then excess ketone was added (200 μL). One of the following was added for its appropriate product, respectively: 2'-methylacetophenone, pinacolone, 2-butanone, and 3-methyl-2-butanone. The mixture was stirred at 70 °C for 12 h to give a red solution. The resulting solution was condensed to 1 mL and then was precipitated with the addition of excess Et₂O. A red solid was collected via centrifugation, which was dissolved in MeOH/MeCN (3 mL/0.3 mL). After filtration, 5 mL of Et₂O was layered onto the filtrate, and red crystals deposited after several weeks. Crystal isolation yields (based on gold): 2c, 40.6 mg, 52%; 2h, 36.3 mg, 47%; 2i, 24.3 mg, 32%; 2j, 48.4 mg, 63%.

Physical Measurements. FT-IR spectra were recorded from KBr pellets in the range 4000–400 cm⁻¹ with a Nicolet AVATAR FT-IR360 spectrometer. All the NMR data were recorded on a Bruker Avance II spectrometer (400 MHz), Avance III spectrometer (500 MHz), and Ascend 500 and 600 MHz magnets. Chemical shifts, δ's, are reported relative to the external standard (85% H₃PO₄ for ³¹P NMR). Mass spectra of complex 5 were recorded on an ESI-TOF mass spectrometer (Agilent Technologies). EDX analysis for 1 was recorded by a HITACHI S-4800 SEM. Elemental analyses were carried out with a Vario EL III elemental analyzer. All the samples are dried in a vacuum oven at room temperature overnight.

X-ray Crystallography. Intensity data were collected using an Oxford Gemini S Ultra diffractometer at 173 K with a Mo Kα (λ = 0.710 69 Å) microfocus X-ray source for clusters 3 and 2a,b,d,g,j. Intensity data were collected using an Oxford Gemini S Ultra diffractometer at 100 K with a Mo Kα (λ = 0.710 69 Å) microfocus X-ray source for cluster 2e. Intensity data were collected using an Oxford Gemini S Ultra diffractometer at 173 K with a Cu Kα (λ = 1.541 84 Å) microfocus X-ray source for cluster 2c. Intensity data were collected using an Agilent SuperNova diffractometer at 100 K with a Mo Kα (λ = 0.710 69 Å) microfocus X-ray source for clusters 2f and 2h. Intensity data were collected using an Agilent SuperNova diffractometer at 100 K with a Cu Kα (λ = 1.541 84 Å) microfocus X-ray source for clusters 2i and 4. The data were processed using CrysAlisPro (multiscan). The 2a molecule was on a 4-fold axis, resulting in the disorder of the methyl carbon and the oxygen of the deprotonated acetone CH₃COC³⁻. Several geometric and displacement restraints were applied to solvent molecules, disordered BF₄ anions, and aromatic rings of phosphine ligands. Non-hydrogen atoms except solvent molecules, counteranions, and the disordered carbon atom and oxygen atom in 2a were refined anisotropically by least-squares on F² using the SHELXTL program. The hydrogen atoms of organic ligands were generated geometrically, while no attempt was made to locate hydrogen atoms of solvent molecules. Compounds 2a–c,f,h–j and 4 have solvent accessible voids due to a large number of disordered solvent molecules. Parts of the counteranions in 2b and 2c could not be resolved due to the weak diffraction data and disorder, but they were included in molecular formulas as requested by charge balance.

Computational Details. The studied system was fully optimized using the B3LYP density functional method with the Gaussian 09 program. The basis set for C, H, O, N, and P was 6-31G*. The valence electrons and core electrons of Au and Ag were described by LanL2DZ and its effective core potential.⁵²

■ ASSOCIATED CONTENT

📄 Supporting Information

Crystal data (CIF) and experimental details. This material is available free of charge via the Internet at <http://pubs.acs.org>.

■ AUTHOR INFORMATION

Corresponding Author

*E-mail: qmwang@xmu.edu.cn.

Notes

The authors declare no competing financial interest.

■ ACKNOWLEDGMENTS

This work was supported by the 973 program (2014CB845603), and the Natural Science Foundation of China (21125102, 21390390, 21473139). We thank D.-e. Jiang from University of California at Riverside for polishing the English.

■ REFERENCES

- Wencel-Delord, J.; Glorius, F. *Nat. Chem.* **2013**, *5*, 369–375.
- Labinger, J. A.; Bercaw, J. E. *Nature* **2002**, *417*, 507–514.
- Gaillard, S.; Cazin, C. S. J.; Nolan, S. P. *Acc. Chem. Res.* **2012**, *45*, 778–787.
- O'Reilly, M. E.; Fu, R.; Nielsen, R. J.; Sabat, M.; Goddard, W. A., III; Gunnoe, T. B. *J. Am. Chem. Soc.* **2014**, *136*, 14690–14693.
- Hashmi, A. S. K.; Hutchings, G. J. *Angew. Chem., Int. Ed.* **2006**, *45*, 7986–7936.
- Hashmi, A. S. K. *Chem. Rev.* **2007**, *107*, 3180–3211.
- Fürstner, A.; Davies, P. W. *Angew. Chem., Int. Ed.* **2007**, *119*, 3410–3449.
- Hashmi, A. S. K.; Rudolph, M. *Chem. Soc. Rev.* **2012**, *41*, 2448–2462.
- Boorman, T. C.; Larrosa, I. *Chem. Soc. Rev.* **2011**, *40*, 1910–1925.
- Boogaerts, I. I. F.; Nolan, S. P. *J. Am. Chem. Soc.* **2010**, *132*, 8858–8859.
- Boutadla, Y.; Davies, D. L.; Macgregor, S. A.; Poblador-Bahamondeb, A. I. *Dalton Trans.* **2009**, 5820–5831.
- Wei, W.; Shao, Y.; Hu, H.; Zhang, F.; Zhang, C.; Xu, Y.; Wan, X. *J. Org. Chem.* **2012**, *77*, 7157–7165.
- Xu, K.; Fang, Y.; Yan, Z.; Zha, Z.; Wang, Z. *Org. Lett.* **2013**, *15*, 2148–2151.
- Xiao, Y.-P.; Liu, X.-Y.; Che, C.-M. *Angew. Chem., Int. Ed.* **2011**, *50*, 4937–4941.
- Yao, X.-Q.; Li, C.-J. *J. Am. Chem. Soc.* **2004**, *126*, 6884–6885.
- Hashmi, A. S. K.; Schafer, S.; Wolffe, M.; Gil, C. D.; Fischer, P.; Laguna, A.; Blanco, M. C.; Gimeno, M. C. *Angew. Chem., Int. Ed.* **2007**, *46*, 6184–6187.
- For an earlier example of the direct auration of acetone in the presence of Ag₂O as a base, see: Nesmeyanov, A. N.; Grandberg, K. I.; Dyadchenko, V. P.; Lemenovskii, D. A.; Perevalova, E. G. *Izv. Akad. Nauk SSSR Ser. Khim.* **1974**, 1206–1212 CAN 81:49772..
- Gasparini, D.; Collado, A.; Gómez-Suárez, A.; Cordes, D. B.; Slawin, A. M. Z.; Nolan, S. P. *Chem.—Eur. J.* **2015**, *21*, 5403–5412.
- Aoyama, Y.; Yamagishi, A.; Tanaka, Y.; Toi, H.; Ogoshi, H. *J. Am. Chem. Soc.* **1987**, *109*, 4735–4737.
- Vicente, J.; Bermudez, M. D.; Chicote, M. T.; Sanchezsantano, M. J. *J. Chem. Soc., Dalton Trans.* **1990**, 1945–1990.
- Lin, Y.-S.; Misawa, H.; Yamada, J.; Matsumoto, K. *J. Am. Chem. Soc.* **2001**, *123*, 569–575.
- Johnson, F. A.; Perry, W. D. *Organometallics* **1989**, *8*, 2646–2650.
- Oertel, A. M.; Ritleng, V.; Busiah, A.; Veiros, L. F.; Chetcuti, M. *J. Organometallics* **2011**, *30*, 6495–6498.
- Foley, N. A.; Gunnoe, T. B.; Cundari, T. R.; Boyle, P. D.; Petersen, J. L. *Angew. Chem., Int. Ed.* **2008**, *47*, 726–730.

- (25) Calhorda, M. J.; Ceamanos, C.; Crespo, O.; Gimeno, M. C.; Laguna, A.; Larraz, C.; Vaz, P. D.; Villacampa, M. D. *Inorg. Chem.* **2010**, *49*, 8255–8269.
- (26) Wang, Q.-M.; Lee, Y.-A.; Crespo, O.; Deaton, J.; Tang, C.; Gysling, H. J.; Gimeno, M. C.; Larraz, C.; Villacampa, M. D.; Laguna, A.; Eisenberg, R. *J. Am. Chem. Soc.* **2004**, *126*, 9488–9489.
- (27) Crystal data for **2a**·2CH₃CN: C₇₅H₆₇B₅N₁₂O₂₀P₄Ag₄Au₄·2CH₃CN, *a* = 22.5062(3) Å, *b* = 22.5062(3) Å, *c* = 11.0208(5) Å, β = 90.00°, *V* = 5582.4(3) Å³, space group P4₂12, *Z* = 2, *T* = 173.0 K, 38 377 reflns measured, 7857 unique (*R*_{int} = 0.1204), final *R*₁ = 0.0844, *wR*₂ = 0.1896 for 5849 obsd reflns [*I* > 2σ(*I*)].
- (28) Yang, Y.; Sharp, P. R. *J. Am. Chem. Soc.* **1994**, *116*, 6983–6984.
- (29) Steigelmann, O.; Bissinger, P.; Schmidbaur, H. *Z. Naturforsch.* **1993**, *48b*, 72–78.
- (30) Schmidbaur, H.; Gabbai, F. P.; Schier, A.; Riede, J. *Organometallics* **1995**, *14*, 4969–4971.
- (31) Vicente, J.; Chicote, M. T.; Guerrero, R.; Jones, P. G. *J. Am. Chem. Soc.* **1996**, *118*, 699–700.
- (32) Scherbaum, F.; Huber, B.; Müller, G.; Schmidbaur, H. *Angew. Chem., Int. Ed. Engl.* **1988**, *27*, 1542–1544.
- (33) Melgarejo, D. Y.; Chiarella, G. M.; Mohamed, A. A.; Fackler, J. P. *J. Z. Naturforsch., B: Chem. Sci.* **2009**, *64*, 1487–1491.
- (34) Koshevoy, I. O.; Haukka, M.; Selivanov, S. I.; Tunik, S. P.; Pakkanen, T. A. *Chem. Commun.* **2010**, *46*, 8926–8928.
- (35) Crespo, O.; Gimeno, M. C.; Laguna, A.; Larraz, C.; Villacampa, M. D. *Chem.—Eur. J.* **2007**, *13*, 235–246.
- (36) Yang, Y.; Ramamoorthy, V.; Sharp, P. R. *Inorg. Chem.* **1993**, *32*, 1946–1950.
- (37) Nesmeyanov, A. N.; Perevalova, E. G.; Struchkov, Yu. T.; Antipin, M. Yu.; Grandberg, K. I.; Dyadchenko, V. P. *J. Organomet. Chem.* **1980**, *201*, 343–349.
- (38) Jin, L.; Weinberger, D. S.; Melaimi, M.; Moore, C. E.; Rheingold, A. L.; Bertrand, G. *Angew. Chem., Int. Ed.* **2014**, *53*, 9059–9063.
- (39) Crystal data for **4**: C₅₄H₅₁B₄N₆O₁₆P₃Ag₃Au₃, *a* = 22.8506(11) Å, *b* = 26.8509(12) Å, *c* = 27.2014(13) Å, β = 108.220(5)°, *V* = 15852.9(13) Å³, space group C2/c, *Z* = 8, *T* = 100.01(10) K, 27 122 reflections measured, 15 235 unique (*R*_{int} = 0.0602), final *R*₁ = 0.1312, *wR*₂ = 0.1187 for 12 419 obsd reflns [*I* > 2σ(*I*)].
- (40) Schmidbaur, H.; Hofreiter, S.; Paul, M. *Nature* **1995**, *377*, 503–504.
- (41) Pei, X.-L.; Yang, Y.; Lei, Z.; Wang, Q.-M. *J. Am. Chem. Soc.* **2013**, *135*, 6435–6437.
- (42) Pauling, L. *The Nature of the Chemical Bond*; Cornell University Press: Ithaca, NY, 1967.
- (43) Schmidbaur, H.; Schier, A. *Chem. Soc. Rev.* **2008**, *37*, 1931–1951.
- (44) Crystal data for **2b**: C₁₆₀H₁₃₈B₁₀N₂₄O₂F₄₀P₈Ag₈Au₈, *a* = 19.5362(3) Å, *b* = 21.4752(3) Å, *c* = 27.3013(4) Å, α = 76.9300(10)°, β = 84.9090(10)°, γ = 80.5750(10)°, *V* = 10 990.8(3) Å³, space group P $\bar{1}$, *Z* = 2, *T* = 173.0 K, 115 965 reflns measured, 50 437 unique (*R*_{int} = 0.0732), final *R*₁ = 0.0849, *wR*₂ = 0.2036 for 30 044 obsd reflns [*I* > 2σ(*I*)]. Crystal data for **2c**·2CH₃CN·H₂O: C₁₆₀H₁₄₁B₁₀N₂₃O₃F₄₀P₈Ag₈Au₈·2CH₃CN·H₂O, *a* = 22.0485(3) Å, *b* = 32.5162(4) Å, *c* = 28.0735(4) Å, β = 97.3590(10)°, *V* = 19 961.0(5) Å³, space group P2₁/n, *Z* = 4, *T* = 172.95(10) K, 98 935 reflns measured, 29 568 unique (*R*_{int} = 0.0761), final *R*₁ = 0.0811, *wR*₂ = 0.1943 for 22 792 obsd reflns [*I* > 2σ(*I*)]. Crystal data for **2d**·4CH₃OH·CH₃CN: C₇₇H₆₈B₅N₁₁O₂F₂₀P₄Ag₄Au₄·4CH₃OH·CH₃CN, *a* = 16.7483(9) Å, *b* = 30.1857(16) Å, *c* = 20.9139(9) Å, β = 96.654(5)°, *V* = 10502.0(9) Å³, space group P2₁/c, *Z* = 4, *T* = 173.0 K, 57 485 reflns measured, 24 027 unique (*R*_{int} = 0.0814), final *R*₁ = 0.0850, *wR*₂ = 0.1925 for 13 435 obsd reflns [*I* > 2σ(*I*)]. Crystal data for **2e**·2CH₃CN·2CH₃OH: C₇₈H₆₆B₅N₁₁O₂F₂₀P₄Ag₄Au₄·2CH₃CN·2CH₃OH, *a* = 16.1973(5) Å, *b* = 16.6308(4) Å, *c* = 20.6296(7) Å, α = 101.403(2)°, β = 93.404(2)°, γ = 115.575(2)°, *V* = 4847.4(3) Å³, space group P $\bar{1}$, *Z* = 2, *T* = 100.0 K, 38 988 reflns measured, 22 171 unique (*R*_{int} = 0.0373), final *R*₁ = 0.0435, *wR*₂ = 0.0921 for 15 998 obsd reflns [*I* > 2σ(*I*)]. Crystal data for **2f**·3CH₃OH: C₁₅₄H₁₃₂B₁₀O₃·
- N₂₄F₄₀P₈Ag₈Au₈·3CH₃OH, *a* = 19.9871(13) Å, *b* = 20.5857(10) Å, *c* = 28.8504(16) Å, α = 94.618(4)°, β = 106.315(5)°, γ = 108.447(5)°, *V* = 10 618.3(10) Å³, space group P $\bar{1}$, *Z* = 2, *T* = 100.01(10) K, 100 348 reflns measured, 43 242 unique (*R*_{int} = 0.0757), final *R*₁ = 0.0770, *wR*₂ = 0.1809 for 32 559 obsd reflns [*I* > 2σ(*I*)]. Crystal data for **2g**·3CH₃CN·2CH₃OH: C₇₅H₆₃B₅N₁₂O₂₀P₄Ag₄Au₄·3CH₃CN·2CH₃OH, *a* = 16.2960(3) Å, *b* = 16.8810(4) Å, *c* = 20.5090(4) Å, α = 100.930(2)°, β = 93.259(2)°, γ = 116.217(2)°, *V* = 4905.93(18) Å³, space group P $\bar{1}$, *Z* = 2, *T* = 173(2) K, 47 816 reflns measured, 22 461 unique (*R*_{int} = 0.0411), final *R*₁ = 0.0438, *wR*₂ = 0.1058 for 17 442 obsd reflns [*I* > 2σ(*I*)]. Crystal data for **2h**: C₁₅₄H₁₄₃B₁₀N₂₄O₂F₄₀P₈Ag₈Au₈, *a* = 17.0945(3) Å, *b* = 22.3918(5) Å, *c* = 26.6588(6) Å, α = 81.141(2)°, β = 83.412(2)°, γ = 82.674(2)°, *V* = 9953.1(4) Å³, space group P $\bar{1}$, *Z* = 2, *T* = 100.01(10) K, 92 371 reflns measured, 46 593 unique (*R*_{int} = 0.0616), final *R*₁ = 0.0958, *wR*₂ = 0.2027 for 25 083 obsd reflns [*I* > 2σ(*I*)]. Crystal data for **2i**·0.5CH₃OH·1.5CH₃CN: C₇₆H₆₉B₅N₁₂O₂₀P₄Ag₄Au₄·0.5CH₃OH·1.5CH₃CN, *a* = 17.2026(9) Å, *b* = 23.0716(14) Å, *c* = 26.8972(12) Å, α = 88.519(4)°, β = 80.909(4)°, γ = 69.262(5)°, *V* = 9853.0(9) Å³, space group P $\bar{1}$, *Z* = 4, *T* = 100.01(10) K, 58 761 reflns measured, 32 745 unique (*R*_{int} = 0.0570), final *R*₁ = 0.0762, *wR*₂ = 0.2097 for 27 751 obsd reflns [*I* > 2σ(*I*)]. Crystal data for **2j**: C₇₅H₇₀B₅N₁₁O₂F₂₀P₄Ag₄Au₄, *a* = 22.0571(6) Å, *b* = 32.6270(12) Å, *c* = 33.4585(12) Å, β = 123.909(2)°, *V* = 19983.4(12) Å³, space group P2₁/c, *Z* = 8, *T* = 172.95(10) K, 78 593 reflections measured, 39 755 unique (*R*_{int} = 0.0682), final *R*₁ = 0.1074, *wR*₂ = 0.2081 for 23 722 obsd reflns [*I* > 2σ(*I*)].
- (45) Ramamoorthy, V.; Sharp, P. R. *Inorg. Chem.* **1990**, *29*, 3336–3339.
- (46) Grandberg, K. I.; Dyadchenko, V. P. *J. Organomet. Chem.* **1994**, *474*, 1–21.
- (47) Vicente, J.; Chicote, M.-T.; Guerrero, R. *Inorg. Chem.* **1997**, *36*, 4438–4443.
- (48) Schmidbaur, H.; Grohmann, A.; Olmos, M. E. *Organogold Chemistry*. In *Gold: Progress in Chemistry, Biochemistry and Technology*; Schmidbaur, H., Ed.; Wiley & Sons Ltd.: Chichester, U.K., 1999; pp 647–746.
- (49) Grohman, A.; Schmidbaur, H. *Gold*. In *Comprehensive Organometallic Chemistry II*; Abel, E. W., Stone, F. G., Wilkinson, G., Eds; Pergamon: Oxford, U.K., 1995; pp 1–56.
- (50) Abdou, H. E.; Mohamed, A. A.; Fackler, J. P., Jr. *Gold(I) Nitrogen Chemistry*. In *Gold Chemistry: Applications and Future Directions in the Life Sciences*; Mohr, F., Ed.; WILEY-VCH Verlag GmbH & Co. KGaA: Weinheim, 2009; pp 1–37.
- (51) Anaya, S. A. S.; Hagenbach, A.; Abram, U. *Polyhedron* **2008**, *27*, 3587–3592.
- (52) Huang, Y. F.; Zhang, M.; Zhao, L. B.; Feng, J. M.; Wu, D. Y.; Ren, B.; Tian, Z. Q. *Angew. Chem., Int. Ed.* **2010**, *53*, 2353–2357.